Published in final edited form as:
J Biomech. 2010 August 10; 43(11): 2106–2113. doi:10.1016/j.jbiomech.2010.04.002.

Dynamic In Vivo Quadriceps Lines-of-Action

Nicole A. Wilson, Ph.D.[1] and **Frances T. Sheehan, Ph.D.**[1]
[1]Functional and Applied Biomechanics Section, Rehabilitation Medicine Department, National Institutes of Health, Bethesda, MD

Abstract

Tissue stresses and quadriceps forces are crucial factors when considering knee joint biomechanics. However, it is difficult to obtain direct, *in vivo*, measurements of these quantities. The primary purpose of this study was to provide the first complete description of quadriceps geometry (force directions and moment arms) of individual quadriceps components using *in vivo*, 3D data collected during volitional knee extension. A secondary purpose was to determine if 3D quadriceps geometry is altered in patients with patellofemoral pain and maltracking. After obtaining informed consent, cine-phase contrast (PC) MRI sets (x,y,z velocity and anatomic images) were acquired from 25 asymptomatic knees and 15 knees with patellofemoral pain during active knee extension. Using a sagittal-oblique and two coronal-oblique imaging planes, the origins and insertions of each quadriceps line-of-action were identified and tracked throughout the motion by integrating the cine-PC velocity data. The force direction and relative moment (**RM**) were calculated for each line-of-action. All quadriceps lines-of-action were oriented primarily in the superior direction. There were no significant differences in quadriceps geometry between asymptomatic and subjects with patellofemoral pain. However, patellofemoral kinematics were significantly different between the two populations. This study will improve the ability of musculoskeletal models to closely match *in vivo* human performance by providing accurate 3D quadriceps geometry and associated patellofemoral kinematics during dynamic knee motion. Furthermore, determination that quadriceps geometry is not altered in patellofemoral pain supports the use of generalized a knee model based on asymptomatic quadriceps architecture.

INTRODUCTION

Quadriceps forces and tissues stresses are crucial factors when considering knee joint biomechanics, as they are controlling factors in tibiofemoral kinematics, patellofemoral kinematics, and cartilage contact forces. Since it is difficult to obtain direct measurements of *in vivo* forces and stresses, musculoskeletal models are increasingly used to provide estimates of these quantities. However the accuracy of model-based analyses is highly dependent on the quality of input data used to create the model. For example, both the 3D force vectors (Elias and Cosgarea, 2007) and moment arms (Hunter *et al.*, 2009) used to represent the quadriceps muscles can dramatically influence computational output (Delp *et al.*, 1990). Musculoskeletal models have also been used in the study of pathology (Arnold *et al.*, 2001; Besier *et al.*, 2009; Hunter *et al.*, 2009). However, musculoskeletal parameters

Correspondence to: Frances T. Sheehan, PhD National Institutes of Health Building 10 CRC RM 1-1469 10 Center Drive MSC 1604 Bethesda, MD 20892-1604 Phone: 301-451-7585 Fax: 301-451-7536 fsheehan@cc.nih.gov.

CONFLICT OF INTEREST STATEMENT The authors report no potential conflicts.

may be altered in pathology, making it difficult to create accurate models of specific pathologies without *a priori* knowledge of musculoskeletal geometry under pathologic conditions (Elias *et al.*, 2006).

Musculoskeletal models of the knee typically rely on input data from a variety of sources. Quadriceps force directions or lines-of-action have been derived primarily from static, cadaver-based studies (Delp *et al.*, 1990; Farahmand *et al.*, 1998; Garg and Walker, 1990; Herzog and Read, 1993; Powers *et al.*, 1998; van Eijden *et al.*, 1986). While these studies provide valuable data, cadaver-based studies cannot reproduce the complex loading patterns applied to the knee *in vivo*. Quadriceps moment arms are often derived based on skeletal geometry (Besier *et al.*, 2009; Delp *et al.*, 1990; Elias *et al.*, 2006; Shelburne *et al.*, 2004) or obtained from other studies that reduce the quadriceps muscles to a single tendon (Powers *et al.*, 2004; Spoor and van Leeuwen, 1992; van Eijden *et al.*, 1986). Reducing the quadriceps to a single tendon eliminates the ability to assess the 3D dynamics of the knee extensor mechanism. Model performance can be enhanced by incorporating a more complete description of 3D quadriceps geometry (force direction and moment arm of individual quadriceps components) quantified *in vivo*, during volitional knee extension.

The need for high-quality data describing musculoskeletal geometry is magnified when modeling pathology, where generalized assumptions regarding musculoskeletal geometry may lead to large errors. Hunter, et al. (2009) demonstrated that improvements in 3D moment arm estimates were essential for investigating pathology, particularly when predicting joint angular accelerations. Arnold, et al. (2001), in a study of cerebral palsy, noted that variations in muscle attachment locations and changes in musculotendon paths with joint motion influenced the calculation of muscle-tendon lengths. Besier, et al. (2009) used a general model to estimate sagittal-plane quadriceps muscle forces and joint moments in patellofemoral pain (PFP) syndrome. While this model used individualized EMG data to account for variations in muscle recruitment patterns, it did not consider the secondary planes of motion, which play a large role in PFP syndrome and many other pathologies (Elias *et al.*, 2006; Hunter *et al.*, 2009; Makhsous *et al.*, 2004; Sheehan *et al.*, 2009; Wilson *et al.*, 2009a), nor did it incorporate the potential for variations in quadriceps geometry associated with PFP (Lin *et al.*, 2004; Jan *et al.*, 2009). One way of addressing these limitations has been through the use of subject-specific modeling (Elias *et al.*, 2006). However, subject-specific modeling is time-consuming and computationally intensive.

The primary purpose of this study was to provide the first description of quadriceps geometry using *in vivo*, 3D data collected during volitional knee extension. A secondary purpose was to determine if the 3D quadriceps force directions and moment arms were altered in pathology, with specific application to subjects with PFP and maltracking. Determination that the quadriceps geometry is not altered in PFP syndrome would support the use of a generalized knee model based on asymptomatic quadriceps architecture.

METHODS

All participants gave informed consent upon entering this IRB-approved study, followed by a complete history and physical. Asymptomatic subjects were excluded if they had any current or past history of knee pain (regardless of etiology), any history of lower leg abnormality, surgery, or major injury. Subjects with PFP syndrome had a clinical diagnosis of idiopathic anterior knee pain present for at least one year and were included based on previously published inclusion/exclusion criteria (Sheehan *et al.*, 2009). In total 23 asymptomatic volunteers and 11 subjects with PFP syndrome were included in this study. If both knees from a single subject fit the criteria for inclusion into a single group and time permitted, both knees were evaluated (Sheehan *et al.*, 2009), resulting in 25 asymptomatic

knees and 15 knees with PFP syndrome being included in the study. Demographic characteristics from the two cohorts were similar, except for gender (Table 1).

Using a previously published imaging protocol (Wilson and Sheehan, 2009), a sagittal-oblique and two coronal-oblique dynamic cine phase contrast (PC) MR image sets (x, y, z velocity and anatomic images over 24 time frames) along with a dynamic cine MR image set (anatomic images in three axial planes over 24 time frames) were acquired while each subject, laying supine, performed cyclic knee flexion/extension movements from maximum attainable flexion (~50°) to full extension (0°). The standard MR image planes (axial, sagittal and coronal) were defined relative to a fixed coordinate system within the MRI. Using an oblique imaging plane (a plane rotated away from the true plane) allowed these planes to be aligned with anatomical features, enhancing consistency across subjects (Fig 1 in Wilson and Sheehan, 2009 provides a visual definition of the imaging planes). 3D rigid body rotations and translations (kinematics) of the femur, tibia, and patella were quantified through integration of the sagittal-oblique cine-PC velocity data (Sheehan *et al.*, 1999), with an accuracy of <0.5mm (Sheehan *et al.*, 1998). In a similar manner, the origin of each musculotendon line-of-action (vastus intermedius (VI), rectus femoris (RF), vastus medialis (VM) and vastus lateralis (VL)) was tracked through integration of the coronal-oblique cine-PC velocity data.

Dynamic anatomic cine images were used to establish the patellar and femoral anatomical coordinate systems (Figure 1) and define bony points of interest, including the patellar center of mass (defined as the centroid of the patella) and the insertion of each musculotendon unit onto the patella, as in a previous study (Wilson and Sheehan, 2009). The femoral coordinate system definition was modified from the previous study (Wilson and Sheehan, 2009) in that the femoral superior/inferior axis was aligned with the femoral anatomical axis, as opposed to the femoral mechanical axis. All lines-of-action, relative moments, and patellar kinematics were defined relative to this femoral reference system. The coordinate system and all points of interest were identified in a single time-frame (full extension) of the dynamic images and integration of the cine-PC velocity data was used to track kinematic changes throughout the motion cycle (Sheehan *et al.*, 1999).

The quadriceps muscles have myotendinous junctions which approach the quadriceps tendons through a range of angles (Buford, Jr. *et al.*, 1997), such that the tendon line-of-action (defined as the unit vector from tendon insertion on the patella to its muscular origin) varies across the width of the tendon. Therefore, six lines-of-action were used to characterize the geometry of the four quadriceps tendons (Figure 2). The central quadriceps components, VI and RF, were each characterized by a single line-of-action representing the central muscle fibers (Buford, Jr. *et al.*, 1997). The VI and RF muscular origins were chosen as the center point of each myotendinous junction and both lines-of-action inserted on the patellar apex, defined as the midpoint of the most proximal edge of the patella (Wilson and Sheehan, 2009). For the VM and VL two lines-of-action were defined for each musculotendon unit. VM proximal (VMP) and VL proximal (VLP) represented the most proximal portion of each tendon. VM distal (VMD) and VL distal (VLD) represented the most distal portion of each tendon (Figure 2). The entire curvilinear VM and VL myotendinous junction was manually outlined (in the first frame of the coronal cine-PC images) and the most proximal and most distal points of the outline were identified as the proximal and distal muscular origins. Similarly, three patellar insertion points were identified: the patellar apex and the most medial (PM) and lateral (PL) points on the patella. The VMP and VLP lines-of-action were defined from the patellar apex to the most proximal muscular origin on the VM and VL, respectively. Similarly, the VMD and VLD lines-of-action were defined from PM and PL to the distal VM and VL muscular origins,

respectively. The patellar tendon (PT) line-of-action was defined by the insertion of the tendon into the patella and tibia.

The 3D relative moment vector (**RM-P**) (Krevolin *et al.*, 2004; Wilson and Sheehan, 2009) was calculated as the cross product of the tendon line-of-action and a line connecting the line-of-action to the point about which moments were summed, the patellar center of mass. The relative moment was composed of three components: flexion/extension (**RM-P$_{F/E}$**), tilt (**RM-P$_{Tilt}$**) and spin (**RM-P$_{Spin}$**). A positive spin indicates a patellar rotation that shifts the superior pole of the patella laterally in the coronal plane. These components transform the tendon force into moments acting on the patella in the medial, superior, and anterior directions, respectively. For example, **RM-P$_{F/E}$** transforms the tendon force into a medially directed moment, causing patellar flexion if no other moments are active. The moment of each muscle could then be calculated by multiplying its scalar force by its **RM**. Moment variables (**RM-P** and scalar moment arm) were not normalized since correlations with body size variables (e.g. subject height, epicondylar width) were not demonstrated.

Data were collected in even temporal increments and interpolated to single-degree knee angle increments in order to create population averages. Only the extension (concentric quadriceps contraction) portion was used in the final analysis, as quadriceps geometry and patellofemoral kinematics were not significantly different between flexion and extension. Statistical comparisons using 2-way ANOVA (condition x knee flexion angle) with repeated measures were made for the RF, VI, VMP, VMD, VLP, and VLD lines-of-action, with Bonferonni post-hoc comparisons. Condition had two levels: PFP and asymptomatic. Knee flexion angle was tested at single-degree increments (0–45°). Patellofemoral kinematics (flexion, tilt, spin, and medial, superior, and anterior shift) were also compared between the two populations using a Student's t-test at a knee angle of 10°, based on a previously published definition of patellar maltracking (Sheehan *et al.*, 2009). At 10° knee extension, the knee was in terminal extension (where patellar maltracking is typically most evident). A p-value <0.05 was defined as significant for all comparisons. Sample size and power calculations were also performed (Appendix 1). Finally, to test for the possibility of bias due to inclusion of paired knees and due to gender distribution variations between populations, a further analysis was conducted using only unilateral (only one knee per subject) female data (Asymptomatic: n=10, PFP: n = 9). All trends in quadriceps geometry remained consistent with those of the full population. Thus, all data presented represent the full population.

RESULTS

In all subjects, the quadriceps lines-of-action were oriented primarily in the superior direction and changed little with knee flexion angle, while the PT lines-of-action was oriented in the inferior direction and became more superiorly oriented with increasing knee flexion angle (Figures 3 & 4C–D, Appendix 2). The VLD line-of-action was significantly more superiorly directed than the VLP line-of-action ($p<0.01$, Figure 3C–D), but there was no significant difference in superior orientation between the VMD and VMP lines-of-action.

The force directions for both the VMP and VMD were oriented slightly medially (Figure 3A), while the VLP force direction was significantly more laterally oriented than the VLD ($p<0.01$, Figure 3A–B). The VI, RF, and PT lines-of-action were oriented slightly laterally and did not change with knee flexion angle (Figure 4A–B).

Both VM lines-of-action were oriented in the posterior direction. In asymptomatic subjects, these became more anterior with increasing knee flexion angle (Figure 3E). VMP was significantly more posteriorly directed than the VMD line-of-action ($p<0.05$). The VL, VI, and RF lines-of-action were oriented in the posterior direction and changed little with knee

flexion angle (Figures 3 & 4E–F). The PT line-of-action was also posteriorly oriented, but became more posterior with increasing knee flexion angle (Figure 4E–F).

RM-P and scalar moment arm values for both populations matched closely with previously published results for healthy subjects (Wilson and Sheehan, 2009), with only minor differences due to the use of a slightly altered coordinate system. **RM-P$_{Spin}$** was the largest **RM-P** component for both VMD and VLD. The magnitude of **RM-P$_{Tilt}$** was smaller than **RM-P$_{Spin}$** for both VMD and VLD, and the magnitude of **RM-P$_{F/E}$** was negligible. Therefore, if the patella was at rest, an isolated force in either the VMD or VLD would result primarily in patellar spin and produce negligible extension. For the central quadriceps and the PT, **RM-P$_{F/E}$** was the largest **RM-P** component, while the magnitude of **RM-P$_{Tilt}$** was negligible.

There were no significant differences in quadriceps geometry between asymptomatic and subjects with PFP (Figures 3 & 4, Appendix 2). However, differences in patellar kinematics, relative to the femur, were present between subjects with PFP and the asymptomatic population. In subjects with PFP there was a significant increase in lateral patellofemoral translation ($p=0.039$), lateral tilt ($p=0.035$), and negative spin ($p=0.044$). There were no significant differences in patellofemoral flexion ($p=0.156$), superior ($p=0.342$), or anterior patellar shift ($p=0.196$) between the two populations.

DISCUSSION

This is the first study to describe 3D quadriceps geometry *in vivo* during volitional knee extension. The data provided in the current study will improve the ability of musculoskeletal models to closely match *in vivo* human performance by providing 3D musculotendon lines-of-action, moment arms, and associated patellofemoral kinematics during dynamic knee motion (Appendix 2).

In both the asymptomatic and PFP populations, the medial/lateral force directions of the quadriceps were not evenly balanced. The VI, RF, and VLP force vectors were oriented laterally and were only offset by the medial orientation of the VM line-of-action. Furthermore, both the VMD and VLD lines-of-action had negligible medial/lateral orientation; suggesting that the most distal (or obliquus) portions of the vasti play only a small role in creating medial/lateral patellofemoral translations. These findings contrast with the previous hypothesis that the primary role of the VM obliquus is to stabilize lateral patellar motion near full knee extension (Bose *et al.*, 1980; Goh *et al.*, 1995; Lieb, 1966). The lack of agreement with previous studies is likely due to the choice of patellar insertion point. For example, Goh et al. (1995) simulated the quadriceps lines-of-action in a cadaver study by attaching wires to the patella, but the specific patellar attachment site for each wire was not specified. In the current study the most medial and lateral points on the patella were chosen to correspond with the distal VM and VL lines-of-action (Farahmand *et al.*, 1998). This likely resulted in the patellar insertions being more medial (and lateral) and thus, the lines-of-action being oriented less in the medial (and lateral) directions than in previous *in vitro* studies.

Interestingly, all quadriceps lines-of-action had large tendencies to produce coronal-plane moments (patellar spin). Both the VM and VL had the largest ability to generate spin. Therefore, while many musculoskeletal models have focused on the sagittal plane mechanics of the knee (Besier *et al.*, 2009; Makhsous *et al.*, 2004) and clinical studies have focused on axial-plane knee kinematics (Brossmann *et al.*, 1993; Draper *et al.*, 2009), it is important to consider all three planes of motion when modeling complex structures such as the knee (Elias *et al.*, 2006; Hunter *et al.*, 2009; Sheehan *et al.*, 2010; Wilson *et al.*, 2009a).

These results are supported by findings from Elias, et al. (2006) who emphasized the importance of secondary planes of motion when studying the patellofemoral joint, noting that force imbalance between the VL and the VM would result in greater changes in patellar tilt and spin compared to lateral patellar translation.

Previous literature suggests that in PFP syndrome, a quadriceps force imbalance results in abnormal patellofemoral kinematics (Besier *et al.*, 2009; Dhaher and Kahn, 2002; Farahmand *et al.*, 1998; Wilson *et al.*, 2009b), which leads to increased joint stress and pain (Fulkerson, 2002; Besier *et al.*, 2009). Implicit in this hypothesis is the assumption that quadriceps geometry is not altered in subjects with PFP syndrome. Gage and Schwartz (2001) suggest that moment arm dysfunction can occur in any traumatic or neuromuscular problem that produces alterations of the bony skeleton. However, alterations of the bony skeleton are not necessary to create moment arm dysfunction. Subtle pathological changes that alter muscular force directions, like muscle architecture changes or injury at the myotendinous junction (Dupuis *et al.*, 2009), could also create moment arm dysfunction. If changes in quadriceps geometry were responsible for the rotational maltracking seen in PFP, increased **RM**s in the lateral tilt and negative spin directions or increased lateral orientation of quadriceps force vectors would be expected. However, the current results demonstrated no significant differences in quadriceps geometry between the two populations; effectively eliminating this as a potential cause of patellar maltracking. Therefore, it is likely that etiology of patellar maltracking is related to an imbalance in the magnitudes of soft tissue forces (Besier *et al.*, 2009) or timing of quadriceps forces (Makhsous *et al.*, 2004). Direct, in vivo, measurements of force from individual muscle components are currently difficult to obtain. However, in order to completely understand the balance of forces between the quadriceps components and its effect on patellar tracking both the magnitude and direction of forces must be further investigated.

Limitations include the fact not all subjects were represented at the extreme ranges of knee flexion/extension, due to individual variations in range-of-motion within the MR scanner. Thus, data points representing five or fewer subjects were eliminated from the total group average. Abrupt slope changes at the extremes of knee flexion angle are due to sudden changes in the number of subjects with available data at these knee flexion angles. Further, all results must be interpreted in light of the coordinate system. Initial data analysis was performed using a common femoral coordinate system (superior/inferior axis aligned with the femoral mechanical axis), which resulted in the mean force directions for all quadriceps components oriented in the lateral, superior, and posterior directions. While consistent with the normal valgus orientation of the knee, a lateral pull from the VM was counter-intuitive from the standpoint of patellofemoral biomechanics. Rotation of the superior/inferior axis, such that it aligned with the femoral anatomical axis (approximately 6° rotation from mechanical axis), restored intuitive force directions (VM had a medial pull while VL had a lateral force direction).

Finally, a previous study demonstrated that small changes in origin and insertion locations (i.e. a single pixel shift in any direction, or the type of error one might expect based on intraobserver variations) altered the scalar moment arm by less than 2% for the VM and VL (Wilson and Sheehan, 2009). However, the VM and VL myotendinous junctions are broad (Farahmand *et al.*, 1998). Therefore, using a single central line-of-action to represent each vastus component may not accurately reflect musculotendon geometry. Results from the current study demonstrate that the transition from the distal to proximal VM and VL lines-of-action alters the scalar moment arm by 36% and 41%, respectively. The potential for population differences in origin and insertion points were not investigated in the current study. However, Jan, et al. (2009) showed that the VMO patellar insertion was more distal (2 mm) on the patella in subjects with PFP, compared to asymptomatic controls. Therefore,

any knee model should be careful to incorporate the appropriate lines-of-action for modeling the conditions of interest.

Caution must be used when applying the current results to future modeling studies. The **RM**s were quantified relative to the patellar center of mass (defined as the centroid of the patella, for the purposes of this study). This was done because the equations involved when summing moments can be simplified when moments are summed about either a fixed point or the center of mass. Numerous modeling studies use other points about which to sum moments (e.g. point of contact). The data from the current study may still be used in such situations by first applying a translation from the patellar center of mass to the point about which moments were summed. Further, the focus of the current study is on tendon orientation derived from tendon and muscle boundaries. Details that affect muscle force output such as fiber orientation cannot be addressed by the current methods. Future studies combining ultrasound and MRI to assess 3D tendon moment arms in the context of subject specific fiber orientations may provide valuable insight into both healthy and pathologic joint biomechanics.

Supplementary Material

Refer to Web version on PubMed Central for supplementary material.

Acknowledgments

This research was supported by the Intramural Research Program of the NIH, and the Clinical Center at the NIH. We thank Abrahm Behnam, Jacqueline Feenster, Bonnie Damaska, and the Diagnostic Radiology Department at the National Institutes of Health for their support and research time. Any opinions, findings, and conclusions or recommendations expressed in this material are those of the authors and do not necessarily reflect the views of the National Institutes of Health or the US Public Health Service.

Reference List

Arnold AS, Blemker SS, Delp SL. Evaluation of a deformable musculoskeletal model for estimating muscle-tendon lengths during crouch gait. Annals of biomedical engineering. 2001; 29:263–274. [PubMed: 11310788]

Besier TF, Fredericson M, Gold GE, Beaupre GS, Delp SL. Knee muscle forces during walking and running in patellofemoral pain patients and pain-free controls. Journal of Biomechanics. 2009; 42:898–905. [PubMed: 19268945]

Bose K, Kanagasuntheram R, Osman MBH. Vastus medialis oblique: An anatomic and physiologic study. Orthopedics. 1980; 3:880–883.

Brossmann J, Muhle C, Schroder C, Melchert UH, Bull CC, Spielmann RP, Heller M. Patellar tracking patterns during active and passive knee extension: evaluation with motion-triggered cine MR imaging. Radiology. 1993; 187:205–12. [PubMed: 8451415]

Buford WL Jr. Ivey FM Jr. Malone JD, Patterson RM, Peare GL, Nguyen DK, Stewart AA. Muscle balance at the knee--moment arms for the normal knee and the ACL-minus knee. IEEE Transactions in Rehabilitation Engineering. 1997; 5:367–379.

Delp SL, Loan JP, Hoy MG, Zajac FE, Topp EL, Rosen JM. An Interactive Graphics-Based Model of the Lower-Extremity to Study Orthopedic Surgical-Procedures. IEEE Transactions in Biomedical Engineering. 1990; 37:757–767.

Dhaher YY, Kahn LE. The effect of vastus medialis forces on patello-femoral contact: a model-based study. Journal of Biomechanical Engineering. 2002; 124:758–767. [PubMed: 12596645]

Draper CE, Besier TF, Santos JM, Jennings F, Fredericson M, Gold GE, Beaupre GS, Delp SL. Using real-time MRI to quantify altered joint kinematics in subjects with patellofemoral pain and to evaluate the effects of a patellar brace or sleeve on joint motion. Journal of Orthopeadic Research. 2009; 27:571–577.

Dupuis CS, Westra SJ, Makris J, Wallace EC. Injuries and conditions of the extensor mechanism of the pediatric knee. Radiographics. 2009; 29:877–886. [PubMed: 19448122]

Elias JJ, Bratton DR, Weinstein DM, Cosgarea AJ. Comparing two estimations of the quadriceps force distribution for use during patellofemoral simulation. Journal of Biomechanics. 2006; 39:865–872. [PubMed: 16488225]

Elias JJ, Cosgarea AJ. Computational modeling: an alternative approach for investigating patellofemoral mechanics. Sports Medicine & Arthroscopy Reviews. 2007; 15:89–94.

Farahmand F, Senavongse W, Amis AA. Quantitative study of the quadriceps muscles and trochlear groove geometry related to instability of the patellofemoral joint. Journal of Orthopeadic Research. 1998; 16:136–143.

Fulkerson JP. Diagnosis and treatment of patients with patellofemoral pain. American Journal of Sports Medicine. 2002; 30:447–456. [PubMed: 12016090]

Gage, JR.; Schwartz, M. Dynamic deformities and lever-arm dysfuntion. Springer Verlag; Heidelberg: 2001.

Garg A, Walker PS. Prediction of total knee motion using a three-dimensional computer-graphics model. Journal of Biomechanics. 1990; 23:45–58. [PubMed: 2307691]

Goh JC, Lee PY, Bose K. A cadaver study of the function of the oblique part of vastus medialis. Journal of Bone & Joint Surgery (Br). 1995; 77:225–231.

Herzog W, Read LJ. Lines of action and moment arms of the major force-carrying structures crossing the human knee joint. Journal of Anatomy. 1993; 182(Pt 2):213–230. [PubMed: 8376196]

Hunter BV, Thelen DG, Dhaher YY. A three-dimensional biomechanical evaluation of quadriceps and hamstrings function using electrical stimulation. IEEE Transactions on Neural Systems & Rehabilitation Engineering. 2009; 17:167–175. [PubMed: 19193516]

Jan MH, Lin DH, Lin JJ, Lin CH, Cheng CK, Lin YF. Differences in sonographic characteristics of the vastus medialis obliquus between patients with patellofemoral pain syndrome and healthy adults. American Journal of Sports Medicine. 2009; 37:1743–1749. [PubMed: 19521000]

Krevolin JL, Pandy MG, Pearce JC. Moment arm of the patellar tendon in the human knee. Journal of Biomechanics. 2004; 37:785–788. [PubMed: 15047009]

Lieb FJ. A Study of Quadriceps Extensor Mechanism at Knee - Anatomical and Mechanical Investigation. Journal of Bone & Joint Surgery (Am) A. 1966; 48:1223–&.

Lin F, Wang GZ, Koh J, Hendrix RW, Zhang LQ. In vivo and noninvasive three-dimensional patellar tracking induced by individual heads of quadriceps. Medicine and Science in Sports and Exercise. 2004; 36:93–101. [PubMed: 14707774]

Makhsous M, Lin F, Koh JL, Nuber GW, Zhang LQ. In vivo and noninvasive load sharing among the vasti in patellar malalignment. Medicine, Science, Sports & Exercise. 2004; 36:1768–1775.

Powers CM, Lilley JC, Lee TQ. The effects of axial and multi-plane loading of the extensor mechanism on the patellofemoral joint. Clinical Biomechanics. 1998; 13:616–624. [PubMed: 11415841]

Powers CM, Ward SR, Chen YJ, Chan LD, Terk MR. The effect of bracing on patellofemoral joint stress during free and fast walking. American Journal of Sports Medicine. 2004; 32:224–231. [PubMed: 14754748]

Sheehan FT, Derasari A, Brindle TJ, Alter KE. Understanding patellofemoral pain with maltracking in the presence of joint laxity: complete 3D in vivo patellofemoral and tibiofemoral kinematics. Journal of Orthopeadic Research. 2009; 27:561–570.

Sheehan FT, Derasari A, Fine KM, Brindle TJ, Alter KE. Q-angle and J-sign: indicative of maltracking subgroups in patellofemoral pain. Clinical Orthopaedics and Related Research. 2010; 468:266–275. [PubMed: 19430854]

Sheehan FT, Zajac FE, Drace JE. Using cine phase contrast magnetic resonance imaging to non-invasively study in vivo knee dynamics. Journal of Biomechanics. 1998; 31:21–26. [PubMed: 9596534]

Sheehan FT, Zajac FE, Drace JE. In vivo tracking of the human patella using cine phase contrast magnetic resonance imaging. Journal of Biomechanical Engineering. 1999; 121:650–656. [PubMed: 10633267]

Shelburne KB, Pandy MG, Anderson FC, Torry MR. Pattern of anterior cruciate ligament force in normal walking. Journal of Biomechanics. 2004; 37:797–805. [PubMed: 15111067]

Spoor CW, van Leeuwen JL. Knee muscle moment arms from MRI and from tendon travel. Journal of Biomechanics. 1992; 25:201–206. [PubMed: 1733995]

van Eijden TM, Kouwenhoven E, Verburg J, Weijs WA. A mathematical model of the patellofemoral joint. Journal of Biomechanics. 1986; 19:219–229. [PubMed: 3700434]

Wilson NA, Press JM, Koh JL, Hendrix RW, Zhang L. In Vivo Noninvasive Evaluation of Abnormal Patellar Tracking During Squatting in Patients with Patellofemoral Pain. Journal of Bone & Joint Surgery (Am). 2009a; 91:558–566.

Wilson NA, Press JM, Zhang LQ. In vivo strain of the medial vs. lateral quadriceps tendon in patellofemoral pain syndrome. Journal of Applied Physiology. 2009b; 107:422–428. [PubMed: 19541742]

Wilson NA, Sheehan FT. Dynamic in vivo 3-dimensional moment arms of the individual quadriceps components. Journal of Biomechanics. 2009; 42:1891–1897. [PubMed: 19515373]

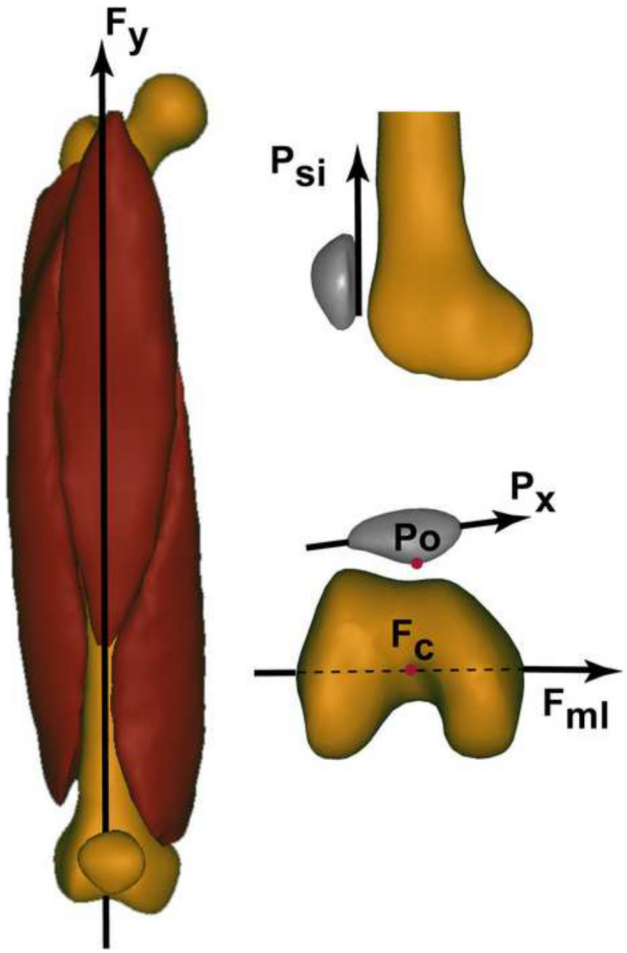

Figure 1. Femoral and Patellar Coordinate Systems

All coordinate systems were defined in the full extension time frame. The femoral y-axis (**Fy**), or superior/inferior axis, was defined as the unit vector in the direction from the center of the femoral epicondyles (point Fc, selected on the axial cine image at the level of the femoral epicondyles) to the rectus femoris musculotendon junction (selected in the cine-PC coronal-oblique image of the rectus femoris), such that **Fy** was aligned with the anatomical axis of the femur. **Fml** was defined as the unit vector in the direction from the lateral to the medial femoral epicondyles (selected on the axial cine image at the level of the femoral epicondyles). The anterior/posterior axis (**Fz**) was defined by the cross product of **Fml** with **Fy**. The femoral x-axis (**Fx**), or medial/lateral axis was defined by the cross product of **Fy** with **Fz**. Fc was defined as the femoral origin. The patellar x-axis (**Px**) was defined as the unit vector connecting the most lateral (PL) and medial (PM) points on the patella (selected on the axial cine image at the mid-patella level – Figure 2). **Psi** was defined as the unit vector along the most posterior edge of the patella (selected on the sagittal-oblique cine-PC image). The anterior/posterior axis (**Pz**), was defined by the cross product of **Px** with **Psi.** The superior/inferior axis (**Py**) was defined as the cross product between **Pz** and **Px.** The patellar origin (Po) was defined as the most posterior patellar point (selected on the axial cine image at the mid-patella level).

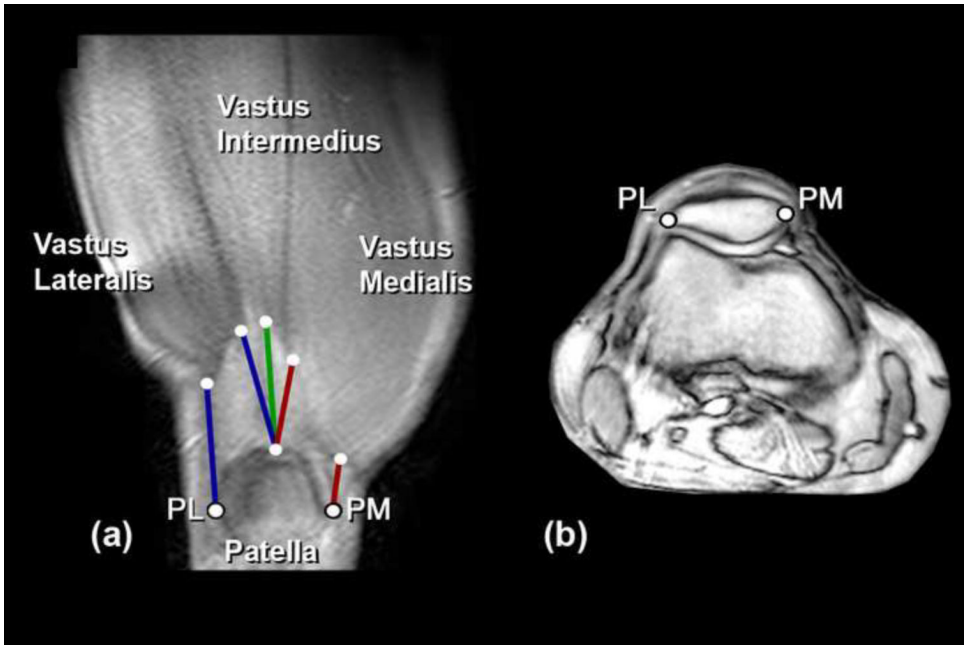

Figure 2.

(a) Anatomic coronal oblique cine-PC image illustrating the corresponding origin and insertion points that define the line-of-action for each musculotendon unit. The imaging plane was aligned parallel to the quadriceps tendon and passed through the myotendinous junction of the vastus intermedius muscle. The myotendinous junctions of the vastus lateralis, vastus intermedius, and vastus medialis muscles can clearly be identified. A similar, but more anterior, imaging plane was used to visualize the mytendinous junction of the rectus femoris (not shown). Moving counter-clockwise in (a): Lines-of-action chosen to represent the vastus medialis muscle are shown in red and represent the distal (VMD) and the proximal (VMP) lines-of-action, respectively. The vastus intermedius line-of-action is shown in green. Lines-of-action for the vastus lateralis muscle are shown in blue and represent the proximal (VLP) and distal (VLD) lines-of-action, respectively. NOTE: Points PM and PL were not chosen from image (a). Rather they were chosen as the most medial and lateral points on the patella from the axial series as illustrated in (b). **(b)** Mid-patellar axial fastcard image taken at full extension using an imaging plane that bisected the patella in the sagittal plane.

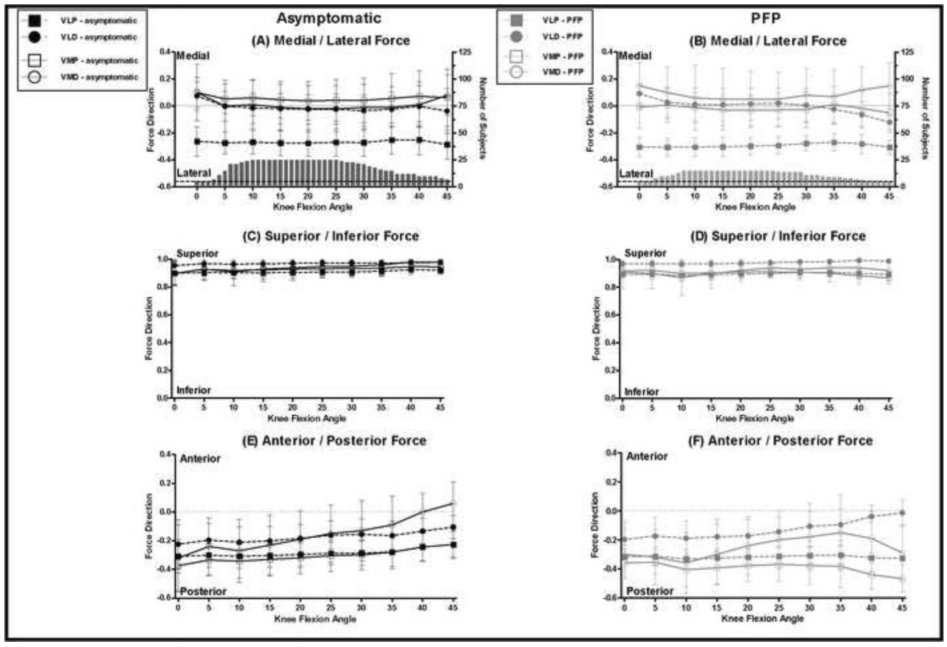

Figure 3. Mean Force Directions for the VM and VL

The projection of the unit force vector in each of the three planes of motion. Lines-of-action associated with asymptomatic subjects (black) are plotted on the left (A, C, E) and lines-of-action associated with subjects with patellofemoral pain (grey) are plotted on the right (B, D, F). In all graphs vastus medialis lines-of-action are shown with solid lines and open symbols while vastus lateralis lines-of-action are shown with dashed lines and filled symbols. Error bars represent one standard deviation. In (A & B) the number of subjects included in each population mean versus knee flexion angle is plotted on the right y-axis.

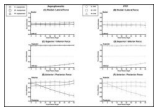

Figure 4. Mean Force Directions for the VI, RF, and PT

The projection of the unit force vector in each of the three planes of motion. Lines-of-action associated with asymptomatic subjects (black, solid line) are plotted on the left (A, C, E) and lines-of-action associated with subjects with patellofemoral pain (grey, dashed line) are plotted on the right (B, D, F). In all graphs the vastus intermedius lines-of-action are shown with open circles, rectus femoris with open squares, and patellar tendon with open triangles. Error bars represent one standard deviation.

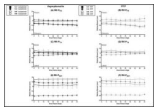

Figure 5. Mean RM-P for VM and VL

RM-P for the vastus medialis (solid lines) and vastus lateralis (dashed lines) muscles. Asymptomatic subjects (black) are plotted on the left and subjects with PFP (grey) are plotted on the right. Asymptomatic subjects are shown with black lines and open symbols and subjects with PFP are shown with red lines and filled symbols. In all graphs vastus medialis **RM**s are shown with solid lines and open symbols while vastus lateralis **RM**s are shown with dashed lines and filled symbols. Error bars represent one standard deviation. (A-B) Mean $\mathbf{RM\text{-}P_{F/E}}$ (positive produces patellar flexion). (C-D) Mean $\mathbf{RM\text{-}P_{Tilt}}$ (positive produces medial patellar tilt). (E-F) Mean $\mathbf{RM\text{-}P_{Spin}}$ (positive, superior pole rotates laterally).

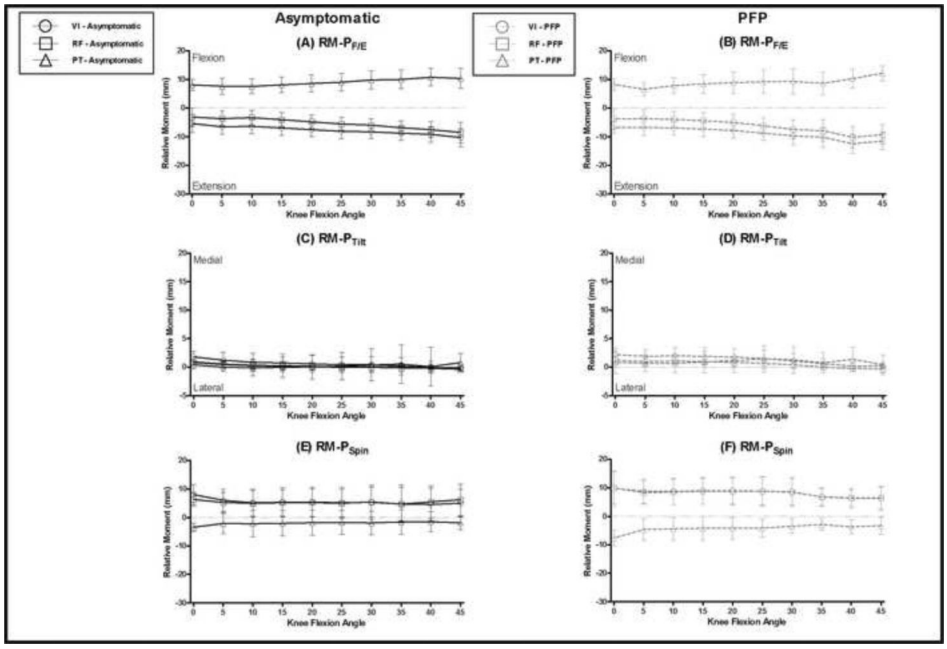

Figure 6. Mean RM-P for VI, RF, and PT

RM-P for the vastus intermedius (open circles), rectus femoris (open squares), and patellar tendon (open triangles). Asymptomatic subjects (black, solid lines) are plotted on the left and subjects with PFP (grey, dashed lines) are plotted on the right. Error bars represent one standard deviation. (A-B) Mean **RM-P$_{F/E}$** (positive produces patellar flexion). (C-D) Mean **RM-P$_{Tilt}$** (positive produces medial patellar tilt). (E-F) Mean **RM-P$_{Spin}$** (positive, superior pole rotates laterally).

Table 1

Subject Demographics

	Asymptomatic	Patellofemoral Pain	p-value
Gender	13 Male, 12 Female	2 Male, 13 Female	0.020
Age (years)	25.1 ± 4.9	27.1 ± 11.8	0.456
Height (cm)	171.2 ± 7.4	178.9 ± 5.8	0.312
Weight (kg)	67.5 ± 12.6	65.6 ± 12.9	0.651
Epicondylar Width (mm)	76.9 ± 6.5	73.9 ± 4.5	0.117